Pore-Scale Modeling Using TOUGH2

Stephen W. Webb and Clifford K. Ho
Sandia National Laboratories
Albuquerque, New Mexico 87185

ABSTRACT

TOUGH2 is a porous media code which is widely-used for simulating flow and transport in fractured and porous media. TOUGH2 is generally employed using REV(Representative Elementary Volume)-size elements or larger volumes. However, because TOUGH2 solves mass, momentum, and energy conservation equations, it can also be used for any size volumes as long as the proper constitutive relationships are included. The present paper discusses application of TOUGH2 to pore-scale modeling of enhanced vapor diffusion in porous media, and the changes and approximations that were employed.

INTRODUCTION

Gas diffusion in porous media is generally significantly smaller than in free space due to the presence of the porous medium. The flow area for gas-phase diffusion is reduced by the presence of the solid particles, by the presence of any liquid, and by the fact that the flow path for diffusion in a porous medium is more tortuous than in free space. Using Fick's law, gas diffusion in a porous media may be expressed as

$$F_i = -\tau\phi S_g D_{12}\rho_g \nabla\omega_i = -\beta D_{12}\rho_g \nabla\omega_i \qquad (1)$$

where D_{12} is the free-space diffusion coefficient at the pressure and temperature of interest. The product of the tortuosity coefficient, τ, the porosity, ϕ, and the gas saturation, S_g, is often referred to as the porous media factor, β. The porous media factor, β, is always much less than 1, and gas diffusion in a porous medium is usually much lower than in free space.

In contrast, it has been postulated that diffusion of a condensible vapor in the presence of its liquid may be considerably enhanced compared to gas diffusion rates and may approach or even exceed free-space values. Enhanced vapor diffusion is discussed in more detail by Ho and Webb (1998) and Webb and Ho (1998). The mechanisms for such an enhancement are postulated occur at the pore scale and include local condensation and evaporation at isolated liquid "islands" within the porous medium, and an increased temperature gradient in the gas phase compared to the average temperature gradient in the equivalent porous medium. As part of their review, Ho and Webb (1998) recommended additional modeling and experiments at multiple length scales, including the pore scale.

MODEL DESCRIPTION

TOUGH2 (Pruess, 1991a) is used to develop a numerical model to investigate the pore-scale processes in enhanced vapor diffusion. The model is described below. More details are given by Webb and Ho (1997).

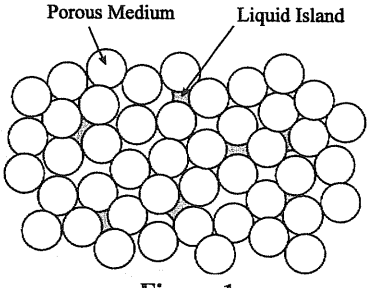

Figure 1
Porous Medium Conceptual Model

Conceptual Model. The conceptual model is depicted in Figure 1. The porous media is a series of randomly-arranged spheres. Heat transfer occurs between the spheres due to particle-to-particle contact, while flow of gas occurs around the spheres and around any liquid islands present. The liquid saturation is assumed to be low such that the liquid is confined to pendular rings, or "liquid islands", and no global flow of liquid occurs. Gas and vapor flow occur due to pressure, temperature, and/or concentration gradients.

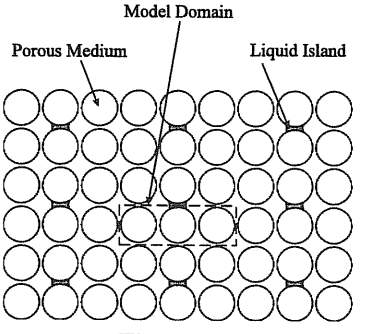

Figure 2
Porous Medium Simplified Representation

Simplified Representation. Figure 2 shows the simplified representation based on the conceptual model. The particles are arranged in rows, and the liquid islands occur on a regular basis. Symmetry is invoked as indicated by the dashed-line box in the figure. A two-dimensional representation has been used, and the solid particles are represented as cylinders.

Numerical Method. TOUGH2 has been slightly modified for the present analysis as discussed below.

1. The flux term for the gas phase is based on the Dusty Gas Model (DGM). Note that the original version of TOUGH2 uses an advective-dispersive formulation. The difference between these two formulations is discussed by Webb (1998a).

2. Some of the phase parameters in the connections have been modified. The standard version assumes that if more than one phase is present in an element, the phases are completely mixed. In the present model, the only elements which contain more than one phase are the elements at the ends of the liquid island, or the interface volumes. For simplicity, the liquid island length is defined so the interface is exactly in the middle of an interface element, and the element is half liquid and half gas. Due to capillary forces and the pore-scale nature of the present model, the phases will be separate, not mixed. The flow path from the interface volume to the gas phase will be entirely gas. Similarly, the flow path between the interface element and the liquid island will be all liquid. The flow path transport parameters used in the code, such as the saturation and fluid transport properties, were modified to reflect separate, rather than mixed, phases.

Model Geometry. Three different geometries were studied:

1) one-dimensional linear system;
2) two-dimension single pore; and
3) two-dimensional pore network.

The use of the one-dimensional linear system allows for a simple evaluation of the effect of the liquid island on the vapor diffusion rate, while the two-dimensional single pore includes the variation in cross-sectional area in a pore. Finally, the two-dimensional pore network considers the competition between vapor diffusion through open pores and through liquid islands. The model parameters, including the nodalization, are discussed in the next section.

MODEL PARAMETERS

The model parameters are summarized in Table 1.

Pore-Scale Dimensions The dimensions for the pore-scale model are consistent with the enhanced vapor diffusion data given by Jury and Letey (1979). For the average value of the capillary head of 300 cm, and using Young-Laplace's equation for the pressure difference across a curved surface, the minimum pore radius is 5 μm.

The cylinders are represented by an octagon (rather than a square) in order to approximate some of the variation of the pore cross-sectional area. A non-symmetrical octagon was employed such that the faces

Table 1
Pore-Scale Model Parameters

Dimensions	
Pore Radius	5 μm
Equivalent Permeability	2×10^{-12} m^2
Particle Radius	50 μm
Model Porosity	0.322
Diffusion	
Binary Diffusion Coefficient	2.42×10^{-5} m^2/s
Knudsen Diffusion Coefficient - Air	1.54×10^{-3} m^2/s
Knudsen Diffusion Coefficient - Vapor	1.96×10^{-3} m^2/s

parallel to the x- and y- directions have a slightly different length than the diagonal faces. This shape allows for the use of a regular grid consisting of square elements except at the diagonal faces of the solid; square elements are desirable when using the 9-point differencing scheme as discussed below. On the diagonal faces, the square elements are divided into two equal triangles, one which is solid and one which is fluid. The particle diameter is 50 μm, which supports the use of square elements, and gives a reasonable model porosity value of 0.322.

The standard version of TOUGH2 employs a 5-point stencil to connect the elements in the x- and y-directions. This numerical scheme is not appropriate for flow along the diagonal surfaces in the model or for flow between the square and triangular elements. Therefore, a 9-point differencing scheme has been used which adds diagonal connections between elements. The main advantage of the 9-point scheme is connections parallel to the diagonal surfaces of the solid particles. As shown by Pruess and Bodvarsson (1983) and Pruess (1991b), grid orientation effects can be significant for the 5-point scheme, especially when a diagonal surface is present; these effects are greatly reduced when a 9-point scheme is employed.

The nodalization of the three models is shown in Figure 3. For simplicity, the boundary elements are not shown. For the one-dimensional linear system, 24 square elements were used including boundary elements on either end of the model; the effective model length is 110 μm (22 active elements x 5 μm). Making use of symmetry, the two-dimensional single-pore model is 24 elements long and 11 elements wide, and the effective model dimensions are 110 μm long by 55 μm wide. Finally, the two-dimensional pore network is 68 elements long and 22 elements wide. The two end columns represent boundary conditions, so the effective dimensions are 330 μm long and 110 μm wide.

Permeability. The analogy between Darcy's law and laminar flow between parallel plates has been used, and the equivalent permeability for the minimum pore dimension of 5 μm is 2×10^{-12} m^2. This analogy

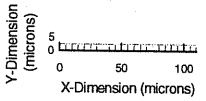

(a) One-Dimensional Linear Model

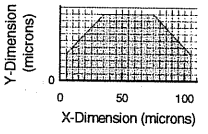

(b) Two-Dimensional Single Pore

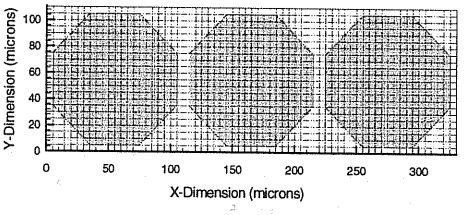

© Two-Dimensional Pore Network

Figure 3
Pore-Scale Models

assumes a parabolic velocity profile between the parallel plates, which is questionable due to the large variation in flow area. This problem has been at least partially addressed by Brown et al. (1995), who calculated velocity profiles between undulating surfaces of a hypothetical fracture. For the present geometry, the results from Brown et al. (1995) indicate that, under steady flow conditions, the fluid velocity profile will be nearly parabolic at the pore throat and "Gaussian" at the wider part of the channel. The fluid velocity is also dependent on the shape of the channel which is not captured in the analogy. Nevertheless, for simplicity, locally parabolic velocity profiles will be implicitly assumed in the present model by relying on the parallel plate analogy. Because the flow modeling is primarily concerned with diffusion, the error introduced through the use of this analogy should be small.

Accepting the parallel plate analogy, the effective permeability must vary normal to the flow direction in order to produce the desired parabolic velocity profile. The effective permeability for a given element can be derived by integrating the velocity profile over the respective coordinates. For an element with coordinates h_1 and h_2 from the center of the channel to the edges of the element, the effective permeability is given by

$$k = \frac{1}{2}\left(\frac{r^2}{4} - \frac{1}{12}\left(h_2^2 + h_1 h_2 + h_1^2\right)\right) \qquad (2)$$

where r is the distance from the centerline of the channel to the solid surface. For any given element, there may be different radii in the horizontal and vertical directions as indicated in Figure 4. Assuming parabolic profiles in both the horizontal and vertical directions, these radii result in different horizontal (h) and vertical (v) effective permeabilities according to the above relationship.

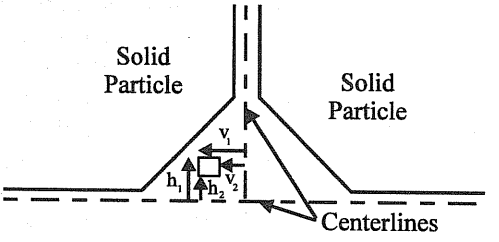

Figure 4
Horizontal and Vertical Effective Permeabilities

Diffusion. The binary diffusion coefficient for the present study is 2.42 x 10^{-5} m^2/s at the analysis conditions of 10^5 Pa and 20°C (Pruess, 1991a). The Knudsen diffusion coefficient is calculated by the following formula from Cunningham and Williams (1980) for perfectly diffuse molecule-wall collisions, or

$$D_\kappa^K = \frac{2}{3} r v \qquad (3)$$

where v is the mean molecular speed

$$v = \left(\frac{8 k_B T}{\pi M_\kappa}\right)^{1/2} \qquad (4)$$

and k_B is Boltzmann's constant. For the minimum pore dimension of 5 μm, the Knudsen diffusion coefficient is 1.54 x 10^{-3} m^2/s for air at 20°C. For water vapor, the value for air is scaled by the inverse of the square root of the ratio of molecular weights, or 1.96 x 10^{-3} m^2/s. No modifications are made to account for the presence of the porous medium.

Similar to the effective permeability, any given element may have different radii in the horizontal and vertical directions. However, as discussed by Cunningham and Williams (1980), the velocity profile due to Knudsen diffusion is independent of distance from the wall. Therefore, the Knudsen diffusion coefficient is simply a function of the horizontal and vertical radii and, unlike the effective permeability, is *not* a function of the local coordinates.

Liquid Island The model for the liquid island is one of the major pieces of the current pore-scale analysis. Capillary pressure across the gas-liquid interface and vapor pressure lowering is included. Capillary pressure is a function of position, or length, of the liquid island; the capillary pressure for a short liquid island is much higher than for a longer liquid island due to the decrease in interface curvature as shown in Figure 5. By geometry, the radius of curvature for a given contact angle can be calculated as a function of liquid island length. For a contact angle of 0°, the capillary pressure as a function of liquid island length is shown in Figure 6, where the coordinate (x) is zero at the minimum pore dimension. A maximum x/R value of 0.75, where R is the particle radius, was used in the development of the capillary pressure function.

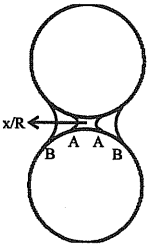

Figure 5
Liquid Island

The capillary pressure due to the gas-liquid interface results in local vapor pressure lowering due to the curvature. For a temperature of 20°C, the saturated water vapor pressure is 2337 Pa. For the maximum capillary pressure of about 30 kPa, the vapor pressure lowering factor is 0.99978, which gives a maximum vapor pressure lowering of only about 0.5 Pa. Even though the magnitude of vapor pressure lowering is small, it can have a large influence on enhanced vapor diffusion as shown by Webb (1998b).

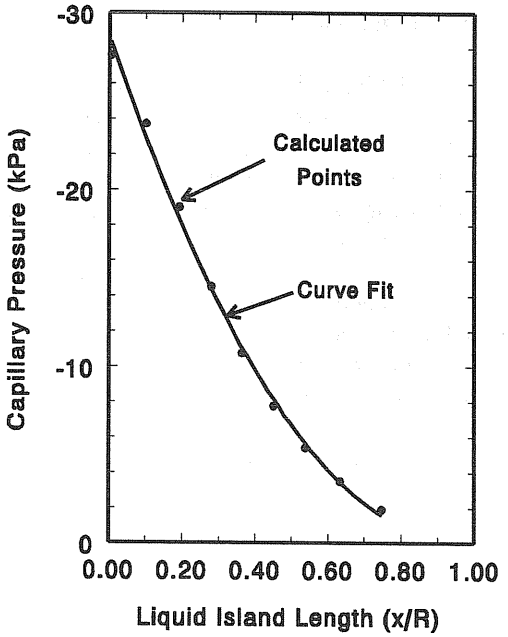

Figure 6
Liquid Island Caoillary Pressure Function

Thermal Conductivity. The thermal conductivity of the gas, liquid, and solid phases are assumed to be 0.025, 0.6, and 2.0 W/m-K, respectively.

Boundary Conditions. The boundary conditions for the problem depend on the gradient imposed. In the results shown in this paper, only a concentration gradient was imposed; the pressure and temperature at both boundaries are the same. These boundary conditions do *not* imply uniform pressure or temperature in the model, rather that a zero gradient was imposed. Webb (in prep.) shows some results including a temperature gradient.

RESULTS

Two-dimensional Pore Network. The two-dimensional pore network is the most general of the three models described in this study. Mass flow vectors for gas-only diffusion, or diffusion without liquid islands, are shown in Figure 7. Because there is no boundary pressure gradient, all flow is due to diffusion. Vapor diffuses from right-to-left, while air diffuses from left-to-right. The mass flux of air is higher than that of water vapor consistent with Graham's law of diffusion as discussed by Webb (1998a).

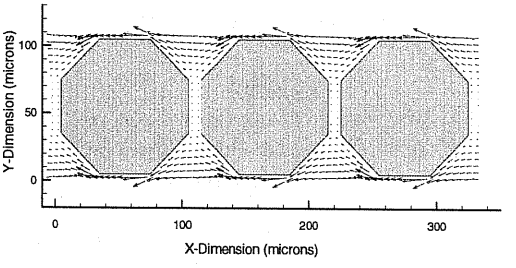

(a) Water Vapor Total Mass Flow Vectors

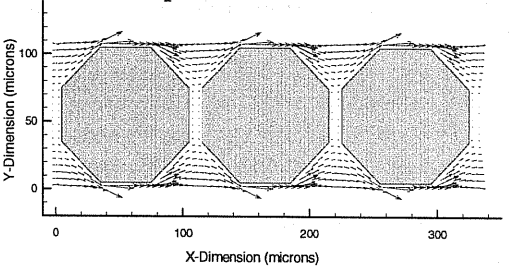

(b) Air Total Mass Flow Vectors

Figure 7
Mass Flow Vectors For All Gas Conditions

A value of the porous media factor, β, can be calculated for the two-dimensional pore model for all-gas conditions. The calculated porous media factor for water vapor is 0.147 compared to Fick's law value in free space, while the porous media factor for air is

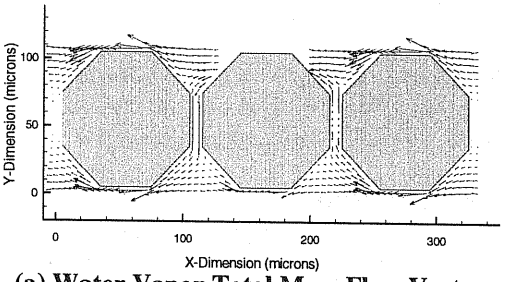

(a) Water Vapor Total Mass Flow Vectors

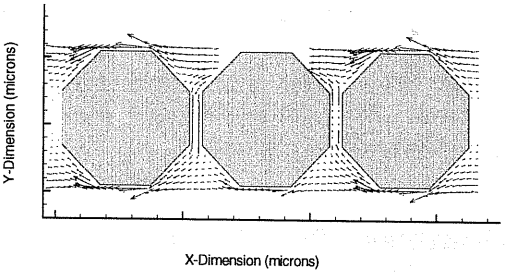

(b) Water Vapor Diffusion Mass Flow Vectors

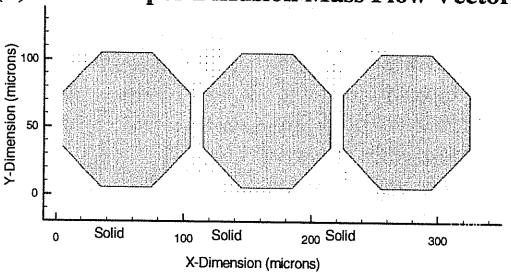

(c) Water Vapor Advection Mass Flow Vectors

Figure 8
Water Vapor Mass Flow Vectors for the Two-Dimensional Pore Network Model For a Liquid Island Length of x/R=0.75

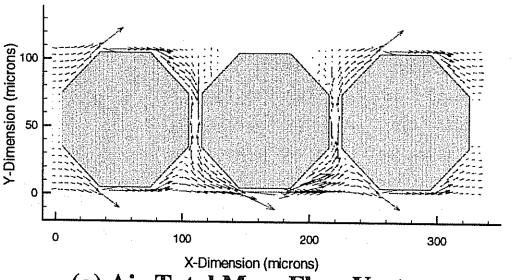

(a) Air Total Mass Flow Vectors

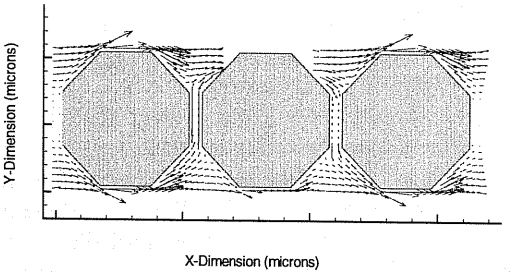

(b) Air Diffusion Mass Flow Vectors

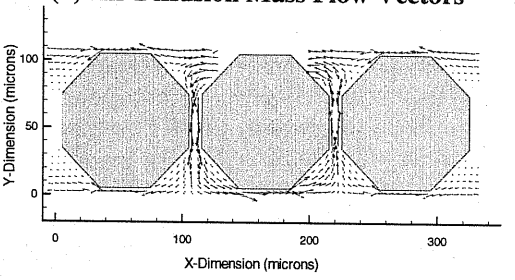

(c) Air Advection Mass Flow Vectors

Figure 9
Air Mass Flow Vectors for the Two-Dimensional Pore Network Model For a Liquid Island Length of x/R=0.75

0.186. The value are different because the present model satisfies Graham's Laws, and the mass flux of air and water vapor are different by the square root of the molecular weights, or a factor of 1.27 (Webb, 1998a). These porous media factors (air and water vapor) are reasonably consistent with the theoretical value predicted by Ryan et al. (1981) of approximately 0.17 and with the experimental data shown by them.

For cases with a liquid island, even though the boundaries have the same total pressure, advection and Knudsen diffusion occur. While vapor essentially flows "through" the liquid island, gas (air) is effectively blocked by the liquid island and builds up on the upstream end of the island. Because air is stagnant at the liquid island, diffusion away from the liquid island caused by the buildup of air must be balanced by advection towards the liquid island. Therefore, there are diffusion, advection, and Knudsen diffusion contributions to vapor and air flow.

Figures 8 and 9 show the mass flow vectors for water vapor and air in the case of the longest liquid island, respectively. The liquid island is assumed to be in the top pore throat of the center particle. Three velocity vectors plots are shown for the total, diffusive, and advective mass velocity contributions using the same scale. Knudsen mass velocity fluxes are not shown since their contribution is small in the present simulations. Vapor essentially diffuses "through" the liquid island via condensation/evaporation mechanisms as indicated by the vector plots. The total vapor mass flow is dominated by diffusive fluxes; the advective contribution is small as indicated by the vector plots. The vapor mass velocity vectors are slightly larger than for the all-gas case indicating enhanced vapor diffusion. For the air, the flow pattern is just about the opposite of the vapor. Since the liquid island effectively blocks air flow, the air must go around the liquid island, and air is stagnant next to the interface. At the right end of the liquid island, vapor diffuses toward the gas-liquid interface; therefore, air diffusion will be opposite and away from the interface. Because air is stagnant, a small pressure gradient will be established to balance

the air diffusive flow rate. This pattern is seen in the velocity vectors. There is a significant advective air flow rate in the middle of the model, especially near the liquid island.

DISCUSSION

The results shown above make qualitative and quantitative sense. For the all-gas case, all the flow is due to diffusion, and the air mass flow rate is slightly greater than the water vapor mass flow rate, consistent with Graham's Law. With a liquid island, vapor pressure lowering causes condensation/evaporation at the liquid island. Air is blocked from flowing through the island, which sets up local counterdiffusion and advection. Overall, the behavior is consistent with gas diffusion principles from the Dusty-Gas Model. It can therefore be concluded that the results make sense and seem reasonable.

CONCLUSIONS

Pore-scale models of enhanced vapor diffusion in porous media have been developed. The detailed results, such as the various mass flow rates and directions, make physical sense. It can therefore be concluded that the pore-scale model developed using TOUGH2 is a reasonable representation of the processes modeled.

One BIG caveat is in order. As noted by Ewing and Gupta (1993), pore-scale modeling is a "useful concept rather than a physical reality". The present authors support this notion.

NOMENCLATURE

D_{12} binary diffusion coefficient for water vapor and air
D^K Knudsen diffusion coefficient
F mass flux
h coordinate measured from the center of the channel
k permeability
k_B Boltzmann's constant
M molecular weight
r pore radius
S saturation
T temperature
v mean molecular speed

Greek

β porous media factor
ρ density
τ tortuosity coefficient
ϕ porosity
ω mass fraction

Subscripts

g gas
κ component

ACKNOWLEDGMENTS

The authors wish to thank Karsten Pruess of Lawrence Berkeley National Laboratory for providing a routine to implement the 9-point differencing scheme used in this analysis. This work was supported by the United States Department of Energy under Contract DE-AC04-94AL85000 as part of a Sandia Laboratory Directed Research and Development Project on Enhanced Vapor-Phase Diffusion in Porous Media. Sandia is a multiprogram laboratory operated by Sandia Corporation, a Lockheed Martin Company, for the United States Department of Energy.

REFERENCES

Brown, S.R., Stockman, H.W. and Reeves, S.J., 1995, "Applicability of the Reynolds equation for modeling fluid flow between rough surfaces," *Geo. Res. Let.*, 22:2537-2540.

Cunningham, R.E., and Williams, R.J.J., 1980, Diffusion in Gases and Porous Media, Plenum Press, New York.

Ewing, R.P., and Gupta, S.C., 1993, "Modeling percolation properties of random media using a domain network," *Water Resourc. Res.*, 29:3169-3178.

Ho, C.K., and Webb, S.W., 1998, "A Review of Porous Media Enhanced Vapor-Phase Diffusion Mechanisms, Models, and Data - Does Enhanced Vapor-Phase Diffusion Exist?" *J. Porous Media*, 1:71-92.

Jury, W.A., and Letey, Jr., J., 1979, "Water Vapor Movement in Soil: Reconciliation of Theory and Experiment," *Soil Sci. Soc. Am. J.*, 43:823-827.

Pruess, K., and G.S. Bodvarsson, 1983, "A Seven-Point Finite Difference Method for Improved Grid Orientation Performance in Pattern Steamfloods," Paper SPE-12252, Seventh Society of Petroleum Engineers Symposium on Reservoir Simulation, San Francisco, CA.

Pruess, K., 1991a, *TOUGH2 - A General-Purpose Numerical Simulator for Multiphase Fluid and Heat Flow*, LBL-29400, Lawrence Berkeley Laboratory.

Pruess, K., 1991b, "Grid Orientation and Capillary Pressure Effects in the Simulation of Water Injection into Depleted Vapor Zones," *Geothermics*, 20:257-277.

Ryan, D., Carbonell, R.G., and Whitaker, S., 1981, "A Theory of Diffusion and Reaction in Porous Media," *AIChE Symposium Series*, 202(77), pp. 46-62.

Webb, S.W., and C.K. Ho, 1997, "Pore-Scale Modeling of Enhanced Vapor Diffusion in Porous Media," *Proceedings of the ASME Fluids Engineering Division*, FED-Vol. 244, pp. 457-468.

Webb, S.W., 1998a, "Gas-Phase Diffusion in Porous Media: Comparison of Models," TOUGH Workshop '98, Lawrence Berkeley Laboratory, May 4-6, 1998.

Webb, S.W., 1998b, "Pore-Scale Modeling of Transient and Steady-State Vapor Diffusion in Partially-Saturated Porous Media," 1998 AIAA/ASME Joint Thermophysics and Heat Transfer Conference, Albuquerque, NM, June 15-18.

Webb, S.W., in prep., "Temperature Gradient Effects in Vapor Diffusion in Partially-Saturated Porous Media."

Webb, S.W. and C.K. Ho, 1998, "Enhanced Vapor Diffusion in Porous Media," TOUGH Workshop '98, Lawrence Berkeley Laboratory, May 4-6, 1998.